



## **PRODUCTION OF COMPOSITE MATERIALS USING HYBRID BIO-NANOPARTICLES IN GUM ARABIC/BANANA PSEUDOSTEM SAP MATRIX FOR PRODUCTION OF AUTOMOBILE BODY PARTS**

**<sup>1</sup>Danladi K. Garba, <sup>2</sup>Emmanuel O. Aweda, <sup>3</sup>Nuhu A. Ademoh, <sup>4</sup>Fredrick Ngolemasango, <sup>5</sup>Pascal A. Ubi, <sup>6</sup>Akor Terngu, <sup>7</sup>Lawal Kabir and <sup>8</sup>Shuaibu O. Yakubu**

<sup>1, 2; 6; 8</sup>Department of Mechanical Engineering, Nigerian Defence Academy, Kaduna, Nigeria.

<sup>3</sup>Department of Mechanical Engineering, Federal University of Technology, Minna, Niger State, Nigeria.

<sup>4</sup>DTR I'M/VMS Materials Development Engineer Wiltshire, United Kingdom

<sup>5</sup>Department of Mechanical Engineering, University of Calabar, Calabar, Cross Rivers State, Nigeria.

<sup>7</sup>Department of Chemical Engineering, Kaduna Polytechnic, Kaduna

**E-mail:** [dkgarba@nda.edu.ng](mailto:dkgarba@nda.edu.ng), [emmanuel.aweda2020@nda.edu.ng](mailto:emmanuel.aweda2020@nda.edu.ng);

**Phone Number:** 080369845454, 08030459602

**DOI:** <https://doi.org/10.5281/zenodo.17158202>

### **Keywords:**

dynamic light scattering, rice husk ash, x-ray diffraction, x-ray fluorescence, thermogravimetric analysis

**Abstract:** This study investigates the development of a bio-based composite for automotive body parts, utilizing nanoparticles derived from banana pseudostem fiber (BPF) and rice husk ash (RHA) using gum Arabic/banana pseudostem sap as matrix. Characterization of the nanoparticles through X-ray fluorescence and X-ray diffraction confirmed BPF was primarily hanksite (72.9%) while RHA was predominantly silica (78.0%), with Dynamic Light Scattering revealing a narrow size distribution (Z-Average of 49.44nm and 34.66nm, respectively). The fabricated composites exhibited superior mechanical properties, with a tensile strength of 2.5 N/mm<sup>2</sup> (control: 2.0 N/mm<sup>2</sup>), flexural strength of 1.9 N/mm<sup>2</sup> (90% higher than the control of 1.0 N/mm<sup>2</sup>) and a significantly enhanced hardness value of 591 N/mm<sup>2</sup>, attributed to effective reinforcement and stress distribution of the nanoparticles. Thermogravimetric analysis confirmed thermal stability up to 61.17°C, while water absorption decreased with reduced fiber content. These findings demonstrate the strong potential of this novel, sustainable composite to meet the performance criteria for both automotive parts and headliner components, valorizing agricultural waste as high-value engineering materials through waste to wealth utilisation.

**Danladi K. Garba, Emmanuel O. Aweda, Nuhu A. Ademoh, Fredrick Ngolemasango, Pascal A. Ubi, Akor Terngu, Lawal Kabir and Shuaibu O. Yakubu**



## 1.0 INTRODUCTION

The automotive industry is undergoing a profound transformation, driven by stringent environmental regulations, the imperative for fuel efficiency, and a growing consumer demand for low cost, high efficiency and sustainable products. A primary strategy for enhancing fuel economy and reducing greenhouse gas emissions is vehicle lightweighting, as a 10% reduction in vehicle weight can result in a 6–8% improvement in fuel efficiency [1]. This has catalyzed extensive research into alternative materials to replace conventional metallic materials, glass fibers and mineral fillers in polymer composites, which are energy-intensive to produce with effects on environment and challenging to recycle.

In this context, natural fiber-reinforced composites (NFRCs) have emerged as a promising class of materials. Derived from renewable resources, materials such as flax, hemp, and jute offer a compelling combination of low density, acceptable specific mechanical properties, biodegradability, and reduced carbon footprint [2]. However, the widespread adoption of NFRCs in structural and semi-structural automotive applications, such as body parts (door panels, trunk liners, bumper beams), is often limited by their inherent variability, susceptibility to moisture absorption, and inferior interfacial adhesion with polymeric matrices compared to synthetic fibers [3].

To overcome these limitations, the need for a paradigm shift involving the use of nanoscale

reinforcements derived from natural sources is desirable. The extraction of nanoparticles, such as cellulose nanocrystals (CNCs) from plant fibers, can significantly enhance the mechanical and thermal properties of the composite due to their high surface area and crystallinity [4]. Simultaneously, the search for sustainable matrix systems has led to the exploration of natural resins. Gum Arabic, a natural biopolymer exudate from Acacia Senegal trees, presents a viable, renewable, and biodegradable alternative to petroleum-based resins, offering good binding properties and low toxicity [5].

This study investigates a novel, fully bio-based composite system designed for automotive body parts. The synergistic use of two agricultural waste products adopted: Banana pseudostem fiber (BPF) nanoparticles and Rice Husk Ash (RHA) nanoparticles, embedded within a Gum Arabic/banana pseudostem sap matrix. Banana pseudostem is a largely untapped waste resource after fruit harvest is a rich source of high-strength cellulose [6]. Its conversion into nanoparticles promises to unlock superior reinforcement potential. Rice Husk Ash, a silica-rich byproduct of rice milling, is valued for its hardness, thermal stability, and ability to act as an effective filler to improve wear and fire resistance [7]. The combination of these nanoscale fillers within a Gum Arabic matrix is hypothesized to create a composite with enhanced mechanical properties, improved thermal stability, and a radically improved environmental profile.

**Danladi K. Garba, Emmanuel O. Aweda, Nuhu A. Ademoh, Fredrick Ngolemasango, Pascal A. Ubi, Akor Terngu, Lawal Kabir and Shuaibu O. Yakubu**



This paper details the extraction and characterization of BPF and RHA nanoparticles, the processing of the hybrid composite, and a comprehensive evaluation of its tensile, flexural, hardness and thermal properties. The findings aim to establish the feasibility of this novel composite material as a sustainable and high-performance alternative for automotive interior and body parts, contributing to the circular economy by valorizing agricultural waste into high-value engineering components.

## 2.0 MATERIALS AND METHODS

The following materials were used in this research work:

1. Nanoparticles of banana pseudostem ash.
2. Nanoparticles rice husk ash (RHA).
3. Nigerian gum Arabic (GA) and banana pseudostem sap (BPS) in a 50-50 mix.

The materials were sourced locally from Kaduna metropolis. Banana pseudostem fibre and rice-husk were then burned under controlled temperature conditions.

Table 1: Table of Materials

SN	Materials	Source
1.	Banana pseudostem fibre and sap	D7, Kurmin Mashi Officer's Quarters, NDA Old site, Ribadu Cantonment, Kaduna.
2.	Rice husk	Alhaji Ahmadu Ali Scorpion Rice Mill, Railway Station Market, Kaduna South, Kaduna.
3.	Gum Arabic	Old Panteka Market, Tudun Nupawa, Kaduna.

## 2.1 METHODS

The methodology for this design is experimental.

## 2.2 PROCEDURE FOR PROXIMATE ANALYSIS OF BANANA PSEUDOSTEM FIBRE AND RICE HUSK SAMPLES

Proximate analysis of banana pseudostem fibre (BPF) and rice husk (RH) samples were carried out using standard gravimetric method of ASTM D-3172.

The materials (BPF and RH) were dried by passing them through nitrogen (N<sub>2</sub>) gas and mass loss was determined. Percentage moisture

content was calculated using the equation below (Composite Materials Handbook, 2002):

$$\%MC = \frac{W_c - D_c}{D_c} * 100 \quad [8] \quad (3.1)$$

Where,

**W<sub>c</sub>** is the weight of air-dried sample, **D<sub>c</sub>** is the weight of oven-dried sample at 103 °C and; **MC** is Moisture content.

## 2.3 PREPARATION AND TREATMENT OF MATERIALS AND PRODUCTION OF SAMPLES

**Danladi K. Garba, Emmanuel O. Aweda, Nuhu A. Ademoh, Fredrick Ngolemasango, Pascal A. Ubi, Akor Terngu, Lawal Kabir and Shuaibu O. Yakubu**

### **2.3.1 Preparation and treatment of Banana pseudo Stem Fibre**

Banana pseudostems obtained from banana plants grown at D7, Kurmin Mashi Officer's Quarters of the Nigerian Defence Academy, Old Site, Kaduna, Nigeria, were cut (Plate 2). The

first three leaf layers were removed to obtain fresh pseudostem. It was then cut longitudinally to separate the pseudostem into smaller pieces and passed through mechanical rollers to extract the sap and produce fibres (Plate 3).



Plate 2: Banana Pseudo stem



Plate 3: Passing banana pseudostem through mechanical rollers to extract sap

The stem fibres were then subjected to water retting by soaking them in water for 24 hours before thoroughly washing them to remove hemicelluloses and lignin from their surfaces. Water retting was carried out to soften the stem, break down pectin (carbohydrate type that holds the fibres together), remove impurities, separate

the fibres and improve their quality. Maceration was performed by soaking the banana fibres in a 5 percent sodium hydroxide (NaOH) solution for 30 mins. Hemicelluloses, lignin, and other components were removed from the fibre by alkali treatment. This alters the structural makeup of cellulose. The natural fibre's (NF) surface roughness of natural fibres is increased by alkali chemical treatment. Consequently, the

**Danladi K. Garba, Emmanuel O. Aweda, Nuhu A. Ademoh, Fredrick Ngolemasango, Pascal A. Ubi, Akor Terngu, Lawal Kabir and Shuaibu O. Yakubu**





polymer and fibre more agglutinated more effectively. After macerating the fibres, were washed with water to neutrality. The banana

fibres were then room-dried for seven days (Plate 4).



Plate 4: Banana Fibres Dried under Room Temperature for Seven Days

The banana fibres were characterised using X-ray fluorescence (XRF) and X-ray diffraction (XRD). The banana fibres were subjected to calcination at approximately 800°C in a muffle furnace after which the banana ash was reduced to nanoparticle size in a ball mill. This study was conducted at the Chemical Engineering Department, Ahmadu Bello University, Zaria. Dynamic Light Scattering (DLS) tests were performed out at the Federal University of Technology, Minna to measure the size distribution and size of the particles.

### **2.3.2 Preparation and Treatment of Rice Husk Ash (RHA)**

The raw rice husks were cleaned and sun dried for eight hours daily for three days. To eliminate impurities and promote better decomposition, then leached in a solution of 5percent hydrochloric acid (HCl). The leached rice husk was carbonised in open air to a temperature of 450°C and then calcinated (decarbonation) in the oven to a temperature of 800°C in a muffle furnace (Plate 5) to produce Rice Husk Ash (RHA). The RHA was filtered using a sieve of size 100 microns to remove impurities.



Plate 5: Furnace (Spectral Laboratories, Kurmin Mashi, Kaduna)

A ball mill was used to produce nanoparticles of the rice husk ash. Dynamic Light Scattering was carried out using Zetasizer nano-particle analyzer to determine the particle size distribution. The size distribution carried out showed that the rice husk ash was in nanoparicles.

The following characterisation processes were carried out: Dynamic Light Scattering (DLS), X-Ray Fluorescence (XRF), X-Ray Diffraction, Thermogravimetric Analysis (TGA) and then

Flexural Strength Test was carried out on the composite material samples produced with rice husk ash nanoparticle as reinforcement and Gum Arabic/Banana Pseudostem sap as matrix material.

### **2.3.3 Preparation and Treatment of Gum Arabic and Banana Pseudostem Sap**

Impurities were removed from Gum Arabic exudates. It was then mixed with banana pseudostem sap using 50:50 ratios (Plates 6a and b). Banana pseudostem sap (Plate 6b) was obtained during the processing of the banana pseudostem. It was sieved to remove impurities.



Plate 6a: Gum-Arabic



Plate 6b: Banana Pseudostem Sap

## 2.4 X-RAY DIFFRACTION

Banana fibre ash and Rice husk ash samples were analyzed using Rigaku MiniFlex 600 X-ray diffraction (XRD) Diffractometer to determine their mineralogical and crystalline composition. The XRD analysis were performed using a standard diffractometer with Cu-K $\alpha$  radiation ( $\lambda = 1.5418 \text{ \AA}$ ). The samples were scanned over a  $2\theta$  range of  $10^\circ$  to  $70^\circ$  with a step size of  $0.02^\circ$  and a counting time of 1 second per step. The resulting diffraction patterns were analyzed using software to identify the crystalline phases and their relative percentages.

## 2.5 X-RAY FLUORESCENCE (XRF)

Table 2: Composite Mix Ratios

S/No.	Sample Name	Gum Arabic and BPS	RHA	Banana Fiber
1	Sample A	30	10	60
2	Sample B	32.5	10	57.5
3	Sample C	35	10	55.0
4	Sample D	37.5	10	52.5
5	Sample E	40	10	50.0

Banana fibre ash and rice husk ash samples were analysed using Genius-IF Xenometric X-Ray Fluorescence (XRF) spectrometer to determine their composition. The XRF were measured over an intensity of 0 to 350 counts per seconds (cps) and a  $2\theta$  range of  $0^\circ$  and  $70^\circ$ .

## 2.6 PRODUCTION OF SAMPLES

Nanoparticles of rice husk ash and banana pseudostem fibre ash were mixed with gum Arabic and banana pseudostem sap (BPS) at various ratios (Table 2). Foil paper was laid inside the wooden mould during production of the samples for easy removal.

**Danladi K. Garba, Emmanuel O. Aweda, Nuhu A. Ademoh, Fredrick Ngolemasango, Pascal A. Ubi, Akor Terngu, Lawal Kabir and Shuaibu O. Yakubu**

*GA/BPS: Gum Arabic/Banana Pseudostem Sap.*

RHA volume fraction was kept constant at 10 percent. The volume fractions of gum Arabic and banana pseudostem fibre are shown in Table 2. The mixtures were thoroughly hand stirred to maintain homogeneity and uniform distribution of the composite. 1000g of each mix was hand layed into a steel mould at room temperature and left to dry/set to produce the composite. The composite material was allowed to set at room temperature. It was removed from the mould once the composite had dried. The composite was sliced according to different test ASTM Standards.

## 2.7 MECHANICAL TESTS

The following mechanical tests were carried out on the composite test samples:

Tensile strength test, flexural strength test, hardness test and thermal test were carried out. 3 pieces of each sample and control samples were produced for the test and an average used. These values were evaluated using SOLID WORKS software after the experiments.

**i. Tensile test:** Universal testing machine was used to determine the amount of strain or elongation needed to break a sample made of polymer composite as well as the force necessary to achieve the stretching or elongation. Tensile strength test samples were prepared according to ASTM D3039 (Figure 3.1). All the dimensions are in millimetres (mm).

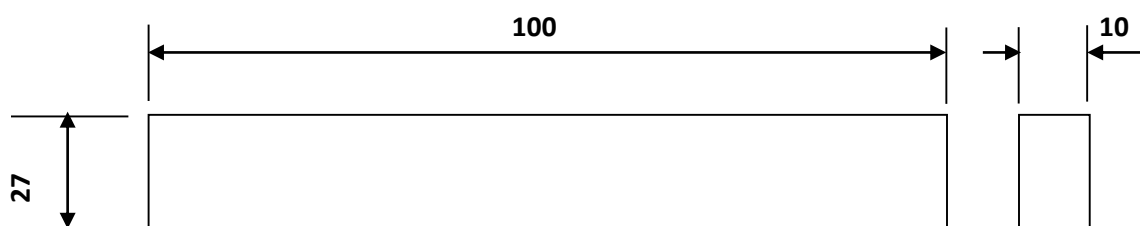


Figure 3.1: **Standard Sample for Tensile Test [8]**

**ii. Flexural Test:** A material's capacity to withstand deformation under load is known as flexural strength. It is a three-point bend test, which favours inter-laminar shear as the failure mode. Utilising Testometric materials testing machine to which a bend fixture was attached,

this test was carried out in accordance with ASTM D7264 standard (Figure 3.2), [9]. The three-point flexural test's flexural strength was calculated using a homogeneous beam Equation (1) as follows;

$$\sigma_f = (3P_{\max} L) / 2bh^2 \quad [9] \quad (1)$$

Where,

**Danladi K. Garba, Emmanuel O. Aweda, Nuhu A. Ademoh, Fredrick Ngolemasango, Pascal A. Ubi, Akor Terngu, Lawal Kabir and Shuaibu O. Yakubu**



$P_{\max}$  = maximum load at failure,  $b$  = specimen width

$h$  = specimen thickness,  $L$  = specimen length between the two support points.

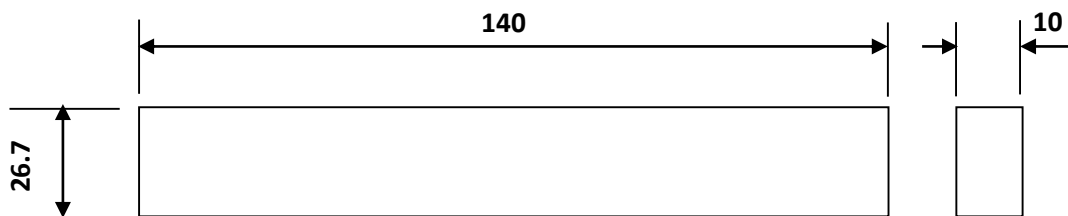


Figure 3.2: Standard Sample for Flexural Test [9]

## 2.8 THERMAL TESTS

Thermogravimetric analysis (TGA) was used to determine thermal characteristics of the composite samples. Their initial weights were approximately 15mg. They were heated from

30°C to 950°C at a rate of 10°C per minute. The rate of deformation and material losses of the samples were observed as temperature increased. Figure 3.3 shows the thermal test sample [8].

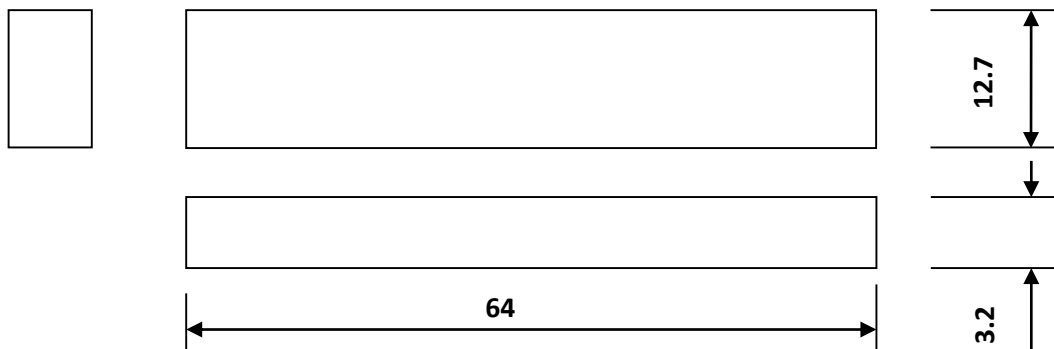


Figure 3.3: Thermal Test Sample [8]

## 2.9 HARDNESS TEST

Brinell method was used to test the composite material samples, because of its polymeric nature (Plate 7). In the Brinell hardness test, an optical method, the size of indentation left by the indenter was measured. The Brinell method uses

a spherical indenter to hit the sample for the test. The larger the indent left in the surface of a work piece (sample) by the Brinell indenter with a defined ball diameter and a defined test force, the softer the tested material.



Plate 7 : Brinell Hardness Testing Machine  
Mechanical Engineering Workshop, NDA,  
Kaduna.)

Brinell hardness (HB) test according to ISO 6506 was carried out using tungsten carbide ball indenter with test load between 1 kgf and 3000 kgf. The Brinell hardness (HB) results from the quotient of the applied test force (F in newtons (N)) and the surface area of the residual indent on the specimen (the projection of the indent) after withdrawing the test force. The measurement was gotten by transforming the physical hit to an electric signal which is then detected by the amplifier and then displayed.

#### **2.10 PERCENTAGE WATER ABSORPTION (PWA)**

A film sample of area 15mm<sup>2</sup> was dried in the oven for three hours at 105°C, cooled, and weighed ( $M_i$ ) immediately. . The sample was then immersed in 100 mL of distilled water at room temperature for 24 hours (ISO 62:2008). It was taken out of the water, wiped with a

smooth cloth, and re-weighed ( $M_f$ ). Three test duplicates were carried out, and the mass changes between the initial and the immersed films were used to determine the PWA using Equation (3).

$$PWA = \frac{M_f - M_i}{M_f} \times 100 \quad [8]$$

Where:

$M_i$ = dry weight and  $M_f$ = wet weight

#### **2.11 THERMOGRAVIMETRIC ANALYSIS (TGA)**

A 15mg weight sample was placed on the sample pan of the Thermogravimetric Analysis (TGA) equipment. It is made up of a furnace inside which is a sample pan supported by a precision balance. That pan was heated from 30°C to 950°C at a rate of 10°C per minute during the experiment and mass of the sample was observed simultaneously. Nitrogen, an inert gas and a sample purge gas was used to control the sample environment. This gas flowed over the sample and comes out through an exhaust.

**Danladi K. Garba, Emmanuel O. Aweda, Nuhu A. Ademoh, Fredrick Ngolemasango, Pascal A. Ubi, Akor Terngu, Lawal Kabir and Shuaibu O. Yakubu**



### **3.0 RESULTS AND DISCUSSION**

#### **3.1 RESULTS**

The following results were obtained.

#### **3.2 CHARACTERISATION OF THE NANOPARTICLES OF BANANA PSEUDOSTEM FIBRE, RICE HUSK AND GUM ARABIC COMPOSITE**

##### **3.2.1 Proximate Analysis of Banana Pseudostem Fibre (BPF)**

Various characterisation methods were used. They are: proximate analysis, dynamic light scattering, X-ray diffraction, X-ray fluorescence and thermogravimetric analysis. The results of these characterisations are presented under this section.

Table 3: Result of Proximate Analysis of Banana Pseudostem Fibre (BPF)

S/N	PARAMETER	BPF	UNIT
1	MOISTURE CONTENT	5.3333	%
2	ASH CONTENT	4.4667	%
3	VOLATILE MATTER	52.6333	%
4	FIXED CARBON	37.5667	%

The moisture content of the banana pseudostem is relatively low, which is a good advantage for storage and handling (Table 3). The ash content indicates the mineral content of the banana fibre. The volatile matter content indicates the

presence of organic compounds that may contribute to its thermal behavior. The high fixed carbon content suggests that the fibre could be suitable for automotive and industrial applications that require a stable carbon source.

##### **3.2.2 Proximate Analysis of Rice Husk (RH)**

Table 4: Result of Proximate Analysis of Rice Husk (RH)

S/N	PARAMETER	RICE HUSK	UNIT
1	MOISTURE CONTENT	4.34	Percent
2	ASH CONTENT	13.44	Percent
3	VOLATILE MATTER	56.96	Percent
4	FIXED CARBON	25.26	Percent

Raw rice husk sample with moderate ash content and high volatiles (Table 2) makes it suitable for

composite applications. Controlled pyrolysis and chemical treatment was used to improve its

**Danladi K. Garba, Emmanuel O. Aweda, Nuhu A. Ademoh, Fredrick Ngolemasango, Pascal A. Ubi, Akor Terngu, Lawal Kabir and Shuaibu O. Yakubu**



performance as nanofiller for biocomposite development.

### 3.2.3 X-Ray Fluorescence (XRF)

Table 5: Results of X-Ray Fluorescence (XRF) Test for Banana Fibre

Banana fibre ash phases	Hanksite	Bischofite	Aluminum Phosphate	Urea	Chaoite
Weight Fraction, wt percent Value	72.9	4.83	3.87	2.87	15.5

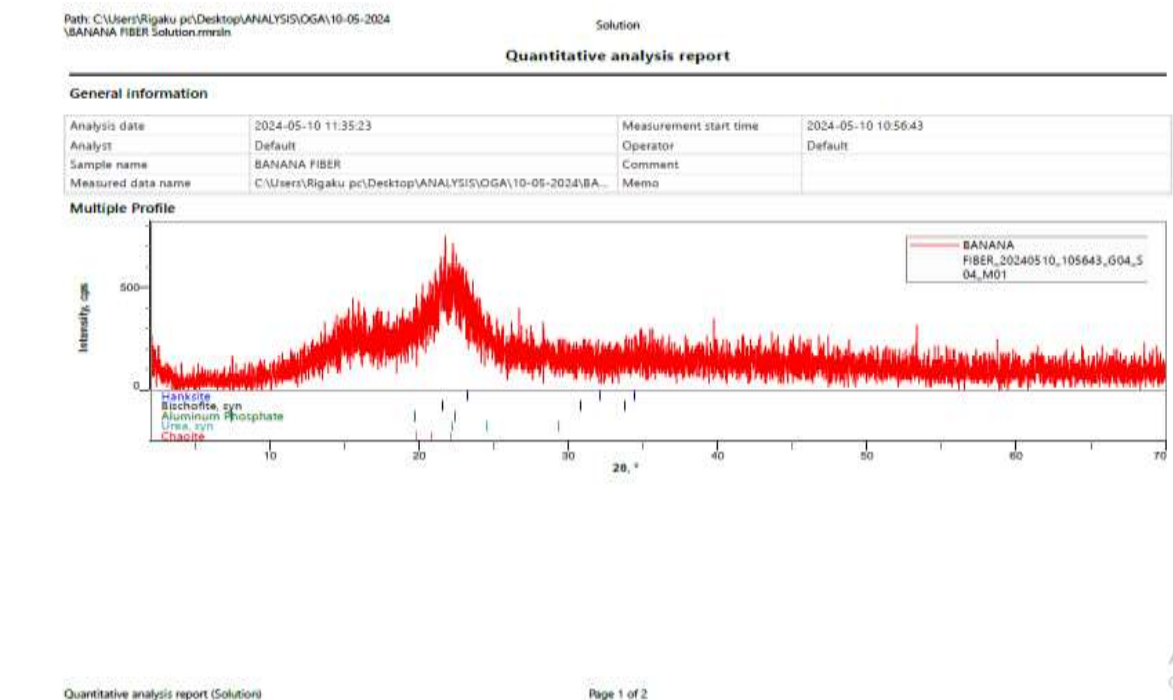


Plate 8: Graph of X-Ray Fluorescence of Banana Pseudostem Fibre Ash

The XRF results indicate that the banana fibre is a natural material with a complex crystalline structure, with hanksite and chaoite as the major components (Table 3). The presence of these

X-Ray Fluorescence (XRF) Results of Banana Pseudostem Fibre Ash is shown in Table 5.

minerals indicates that the fibre has been exposed to a variety of environmental conditions, including high temperatures, saline environments, and acidic conditions (Plate 8).

- The high percentage of hanksite (72.9percent) suggests that this phase is critical

**Danladi K. Garba, Emmanuel O. Aweda, Nuhu A. Ademoh, Fredrick Ngolemasango, Pascal A. Ubi, Akor Terngu, Lawal Kabir and Shuaibu O. Yakubu**





to the overall properties of the fibre, potentially contributing to its mechanical strength and stability.

- The process of heating the banana fibre to ash under high temperature in the oven, or natural exposure of the banana pseudostem to extreme conditions, may be the reasons for the presence of chaoite (15.5percent), which could improve its durability.

Table 6: Results of X-Ray Fluorescence (XRF) Test for Rice Husk Ash

Rice Husk Ash Phases	Silica (Quartz)	Lime	Graphite	Sylvine
Weight Fraction, wt percent Value	78	8.3	7.6	6.3

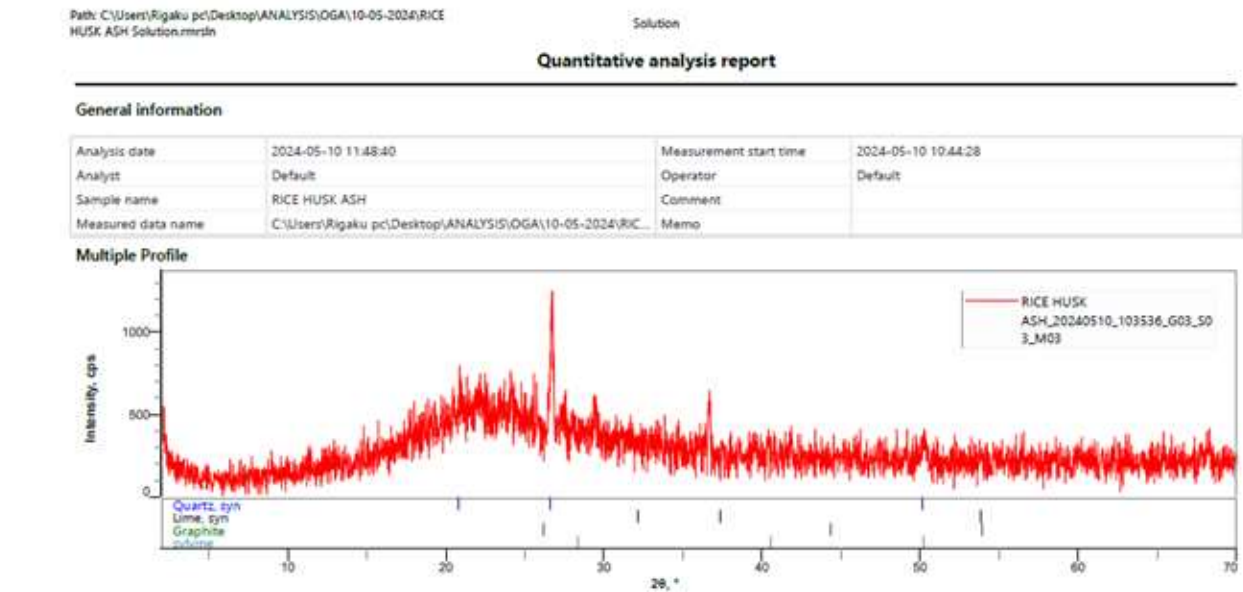


Plate 9: Graph of X-Ray Fluorescence (XRF) of Rice Husk Ash

The XRF analysis revealed the presence of four primary crystalline phases in the nanoparticles of the rice husk ash sample which predominantly

**Danladi K. Garba, Emmanuel O. Aweda, Nuhu A. Ademoh, Fredrick Ngolemasango, Pascal A. Ubi, Akor Terngu, Lawal Kabir and Shuaibu O. Yakubu**



is composed of silica, with significant amounts of lime, graphite, and sylvine (Plate 9) which enhances mechanical properties such as impact strength, tensile strength, flexural strength, and fracture toughness. The result shows that the material is a rich source of silica which makes it suitable for the production of high performance bio-based composite materials.

### 3.2.4 X-Ray Diffraction (XRD)

The results of X-ray Diffraction (XRD) non-destructive test conducted on banana pseudostem fibre ash, focusing on the diffraction peak observed at  $2\theta = 19.04^\circ$  are presented in Table 7.

**Table 7:** Results of X-ray Diffraction (XRD) Test of banana pseudostem fibre ash.

Experimental Details	Measurement Values
$2\theta$ ( $^\circ$ )	19.04
d-spacing (d, Å)	4.66
Peak Height (counts)	80
FWHM ( $^\circ$ )	$10.57^\circ$
Integrated Intensity (counts per second (cps))	898
Integrated Width (Int. W.)	$11^\circ$
Asymmetry	0.80
Decay (nL/mL)	0.00
Decay (nH/mH)	0.00
Crystallite Size (Å)	7.96

*Note: FWHM means Full Width at Half Maximum*

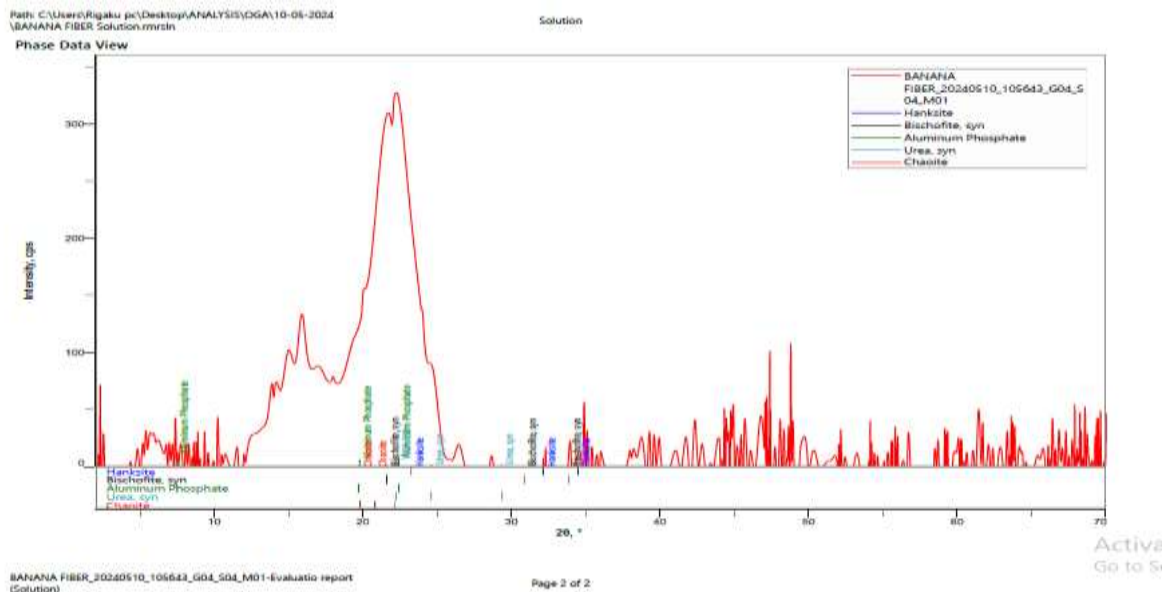


Plate 10: Graph of X-Ray Diffraction of Banana Pseudostem Fibre Ash

XRD analysis of banana pseudostem fibre revealed significant crystalline regions, primarily composed of cellulose, as clearly shown by the diffraction peak at  $2\theta = 19.04^\circ$  and the corresponding d-spacing of  $4.66 \text{ \AA}$  (Plate 10). The high peak height and integrated intensity confirmed the presence of a substantial amount of crystalline material. The Full Width at Half Maximum (FWHM) and crystallite size show that the crystallites are relatively small, which is

consistent with the natural structure of plant fibres. The slight peak asymmetry and absence of decay further supported the stability and well-ordered nature of the crystalline regions. Overall, the XRD results provide valuable insights into the structural properties of banana pseudostem fibre, highlighting their potential for the development of automobile body parts and other engineering applications.

*Qualitative analysis results of the banana pseudostem fibre are shown in Table 8.*

Table 8: Results of Qualitative Analysis of Banana Pseudostem Fibre Ash

Phase name	Formula
Hanksite	$\text{Na}_{22} \text{K Cl (C O}_3)_2 (\text{S O}_4)_9$
Bischofite syn	$\text{Mg Cl}_2 6 \text{ H}_2 \text{ O}$
Aluminum Phosphate Al P O <sub>4</sub>	$\text{Al P O}_4$
Urea syn	$\text{C H}_4 \text{ N}_2 \text{ O}$
Chaoite	C

**Danladi K. Garba, Emmanuel O. Aweda, Nuhu A. Ademoh, Fredrick Ngolemasango, Pascal A. Ubi, Akor Terngu, Lawal Kabir and Shuaibu O. Yakubu**



X-Ray Diffraction (XRD) of rice husk ash is shown in Table 9 and qualitative analysis of RHA in Table 10.

Table 9: Result of X-ray Diffraction (XRD) Test for Rice Husk Ash

Experimental Details	Measurement Values
$2\theta$ (°)	37.81
d-spacing (d, Å)	2.5374
Peak Height (counts)	365
FWHM (°)	0.16°
Integrated Intensity (counts per second (cps))	69.3333
Integrated Width (Int. W.)	0.2233°
Asymmetry	0.5666
Decay (nL/mL)	1.1667
Decay (nH/mH)	0.1333
Crystallite Size (Å)	603.33

*Note: FWHM means Full Width at Half Maximum*

Table 10: Result of Rice Husk Ash Qualitative Analysis

Phase name	Formula
Quartz syn	SiO <sub>2</sub>
Lime syn	CaO
Graphite	C
Sylvine	KCl



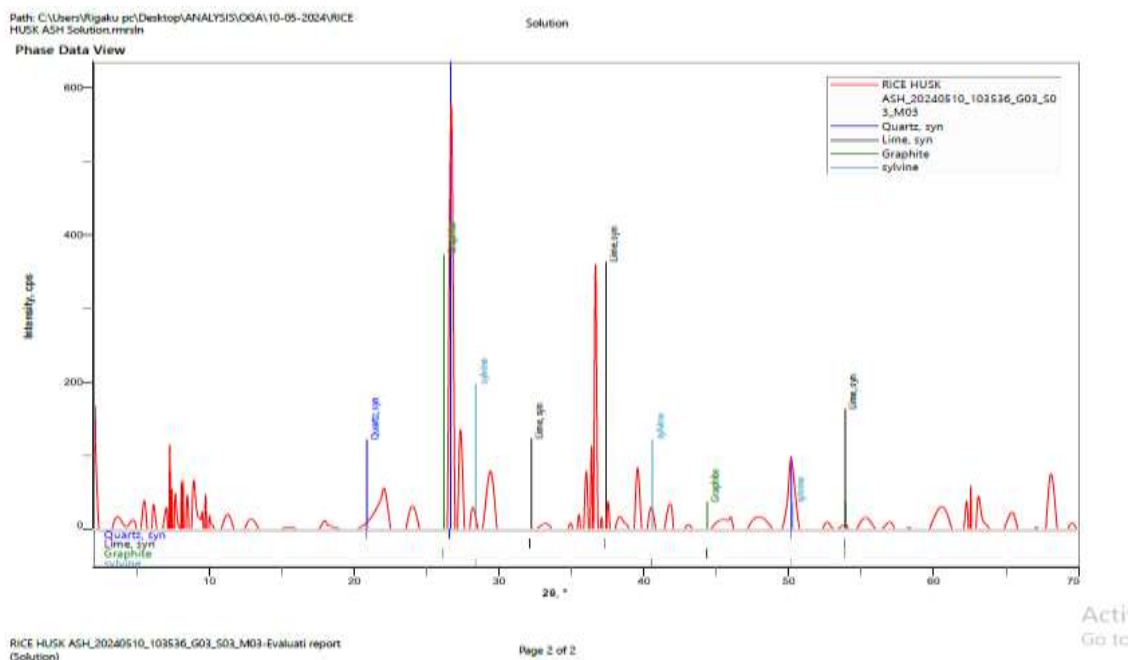


Plate 11: Graph of X-Ray Diffraction (XRD) of Rice Husk Ash

X-Ray Diffraction (XRD) analysis, a non-destructive analytical technique, was used to determine the elemental composition of nanoparticles of the rice husk ash (Plate 11). The analysis provides insights into the crystalline structure and composition of the samples. Table 4 shows the results of the X-ray Diffraction (XRD) nanoparticles of the rice husk ash using Genius-IF Xenometric X-Ray Diffraction (XRD) spectrometer. The diffraction peak position ( $2\theta = 37.81^\circ$ ) shows the presence of a crystalline phase in the nanoparticles of the rice husk ash (Figure 4). This angle corresponds to the d-spacing of  $2.5374 \text{ \AA}$ , which is characteristic of silica ( $\text{SiO}_2$ ) in its crystalline form. The d-spacing value, ( $d = 2.5374 \text{ \AA}$ ) confirms the presence of a

well-defined crystalline structure. This value is consistent with the interplanar spacing of silica phases commonly found in rice husk ash.

The peak height (365 counts) reflects the intensity of the X-ray Diffraction signal. A higher peak height suggests a significant concentration of the crystalline phase in the sample.

The narrow full width at Half Maximum (FWHM =  $0.16^\circ$ ) value shows that the sample has good crystallinity.

The XRD results confirm the presence of crystalline silica phase in the rice husk ash, (Table 4). The narrow Full Width at Half Maximum (FWHM) and large crystallite size indicate a well-ordered crystalline structure with minimal defects. The asymmetry and decay parameters suggest minor instrumental or sample-related effects but do not significantly

**Danladi K. Garba, Emmanuel O. Aweda, Nuhu A. Ademoh, Fredrick Ngolemasango, Pascal A. Ubi, Akor Terngu, Lawal Kabir and Shuaibu O. Yakubu**



impact the overall interpretation. The results demonstrate the potential of nanoparticles of the rice husk ash as a source of high-purity silica for various industrial applications including use for automobile body parts.

### 3.2.5 Dynamic Light Scattering (DLS)

Table 11: Dynamic Light Scattering (DLS) Result of banana fibre ash nanoparticles

Z-Average (nm)	pdi	Intercept	Result Quality
49.44	0.258	0.757	Good

DLS analysis confirmed that the banana pseudostem fibre ash nanoparticles had a well-defined size (~49.44 nm) with moderate monodispersity (PDI: 0.258). The strong correlation signal (intercept: 0.757) and good result quality suggest that the sample preparation and measurement were effective.

Table 12: Dynamic Light Scattering (DLS) Result of Rice Husk Ash Nanoparticles

Z-Average (nm)	pdi	Intercept	Result Quality
34.66	0.204	0.757	Good

The Z-Average (nm) value represents the intensity-weighted mean hydrodynamic diameter of the nanoparticles. A size of 34.66 nm confirms that the size of the rice husk ash nanoparticles lie within the nanometer range (0-100nm), making them suitable for applications in nanocomposites, adsorbents, and catalysts where fine particle sizes are required for enhanced performance. The Polydispersity Index (PDI) value indicates the width of the particle size distribution. A PDI of 0.204 suggests a narrow size distribution, indicating

Zetasizer nano-particle analyzer was used to analyse banana fibre ash and rice husk ash nanoparticles using Dynamic Light Scattering (DLS) process. The results are shown in tables 11 and 12.

These nanoparticles can be used in various nanotechnology applications, including nanocomposites, automobile body parts, biomedical uses, and environmental remediation, where consistent and stable nanoparticle sizes are crucial.

good monodispersity. Since PDI values below 0.7 are considered ideal for uniform nanoparticle dispersion, this result signifies a stable and homogeneous particle population, which is desirable for applications requiring consistent performance.

The classification of the result as "good" indicates that the measurement was conducted under optimal conditions, yielding reliable data. This confirms that the sample preparation and dispersion were effective, minimizing



aggregation and ensuring accurate particle size estimation.

These characteristics make the nanoparticles of rice husk ash suitable for various advanced applications, including automobile parts

production, high performance coating and other composite applications in the industry. Size distribution report of the DLS test is presented in Plate 12.



Plate 12: DLS Size Distribution Report

### 3.2.6 Thermal Test

Results of thermogravimetric analysis are presented in this section.

**Danladi K. Garba, Emmanuel O. Aweda, Nuhu A. Ademoh, Fredrick Ngolemasango, Pascal A. Ubi, Akor Terngu, Lawal Kabir and Shuaibu O. Yakubu**



## Sample A

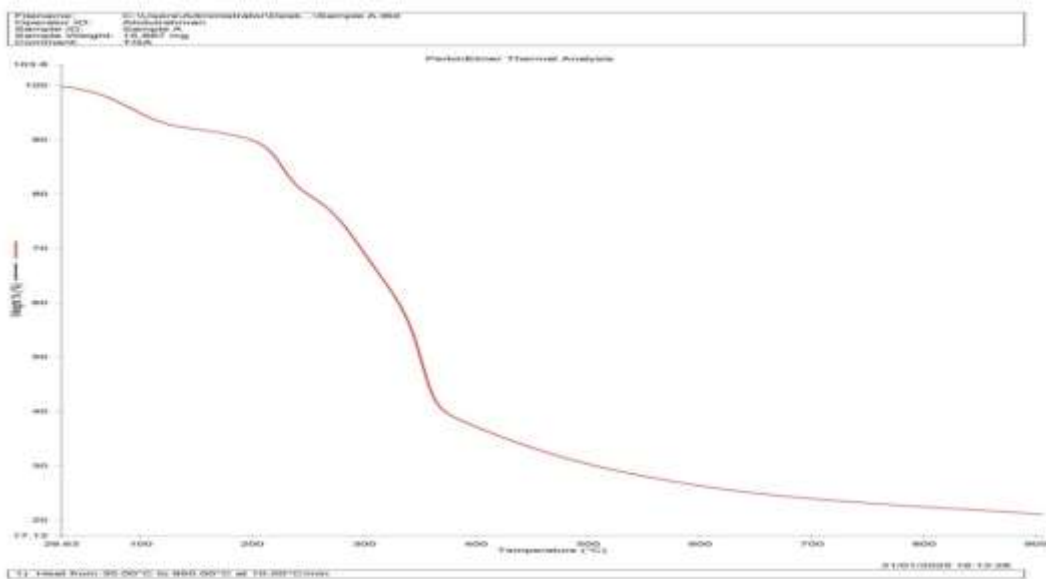


**Plate 13: TGA result of Sample A**

## Sample B

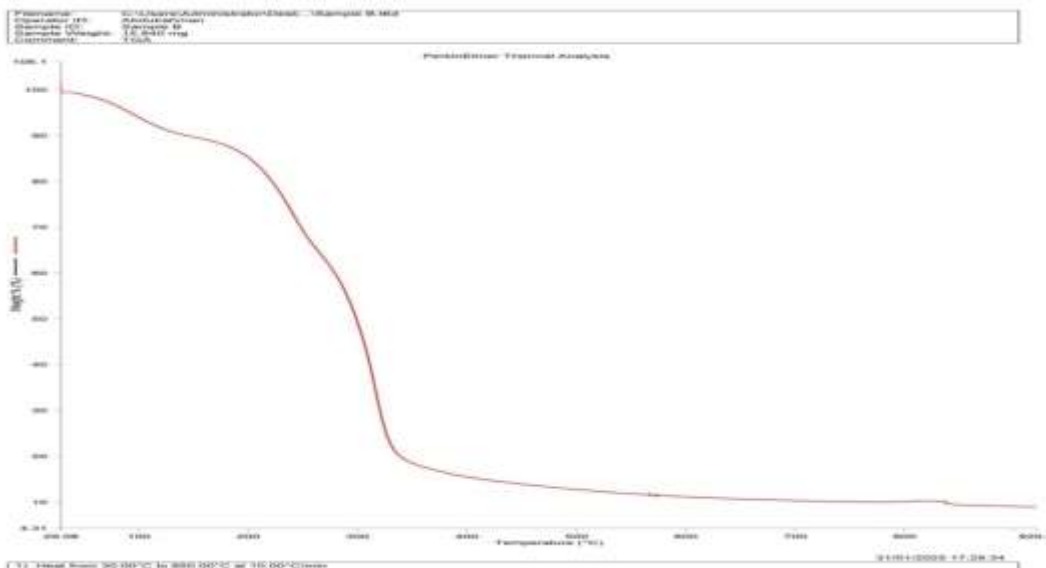


**Plate 14: TGA result of Sample B**

**Danladi K. Garba, Emmanuel O. Aweda, Nuhu A. Ademoh, Fredrick Ngolemasango, Pascal A. Ubi, Akor Terngu, Lawal Kabir and Shuaibu O. Yakubu**



## Sample C

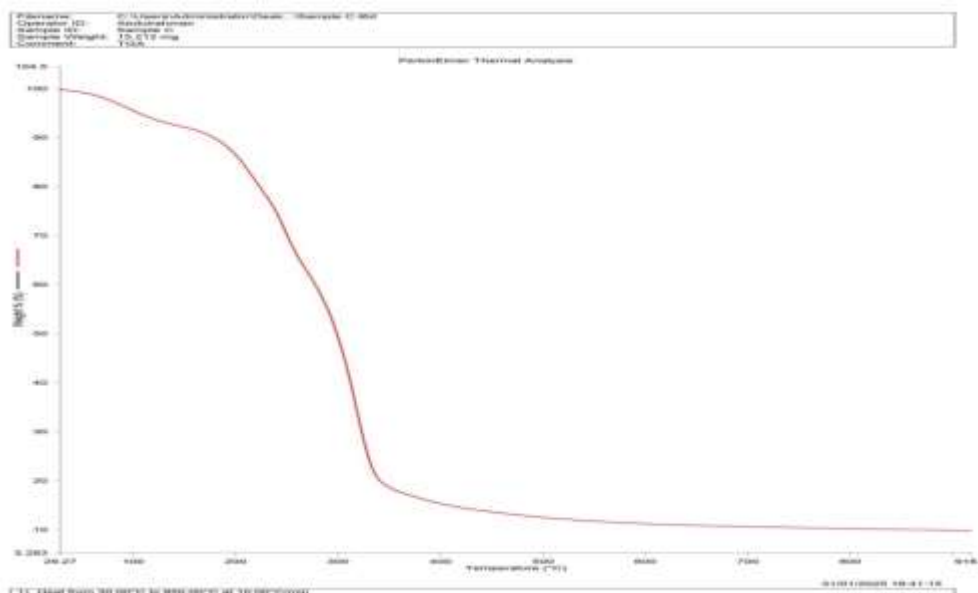


## Plate 15: TGA result of Sample C

### Sample D

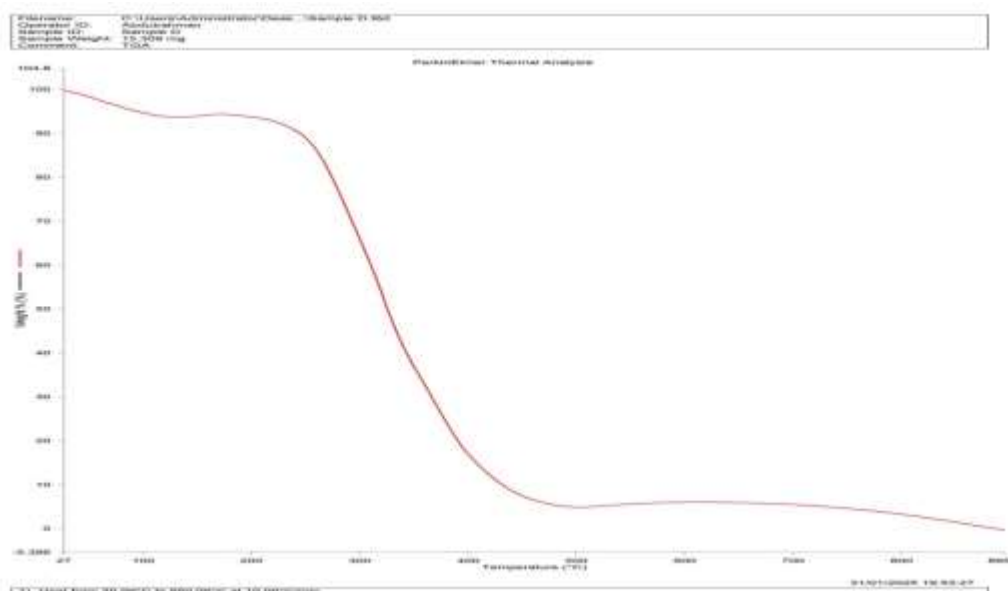


## Plate 16: TGA result of Sample D

**Danladi K. Garba, Emmanuel O. Aweda, Nuhu A. Ademoh, Fredrick Ngolemasango, Pascal A. Ubi, Akor Terngu, Lawal Kabir and Shuaibu O. Yakubu**



## Sample E

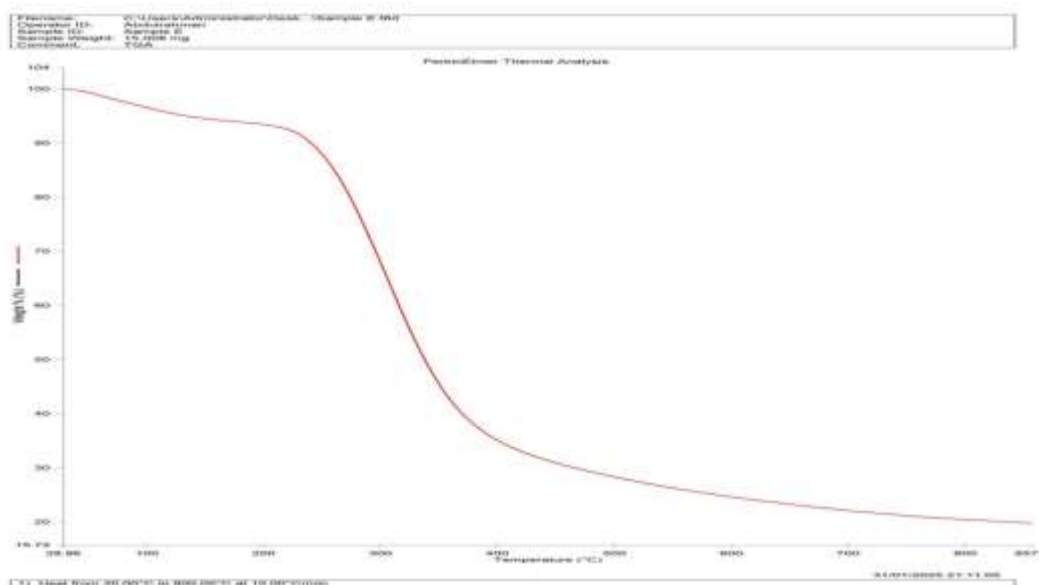


### Plate 17: TGA result of Sample E

The thermal behaviour of the composite samples (approximate weight of 15mg) was analysed using Thermogravimetric Analysis (TGA). They were heated from 30°C to 950°C at a rate of 10°C per minute. Graphs of weight loss against temperature were plotted (Plates 13 to 17).

The composite samples were found to be stable between 0°C to 61.17°C with no degradation or weight reduction. Significant reduction in weight was observed from about 200°C and 400°C for the samples. Samples with higher fibre volume exhibited high decomposition temperatures while samples with lower fibre volume exhibited lower decomposition temperature (Zohuriaan and Shokrolahi, 2003).

The composite was made with rice husk ash nanoparticles as the reinforcing material and gum Arabic as the matrix material. The composite was found to be thermally stable. Sample A with more fibre was found to be more thermally stable than samples B and C with less fibre material. Hence, the choice of sample A, because fibre content create barriers to heat flow in composites. The samples with lower fibre content have fewer barriers, the fewer the barriers, the higher the heat flow. Thereby, increasing their deformation rate.

### 3.3 MECHANICAL PROPERTIES TESTS

#### 3.3.1 Tensile Tests

Tensile test graph of gum Arabic/banana sap matrix reinforced with banana fibre and rice husk ash nanoparticles are presented in Figure 1.

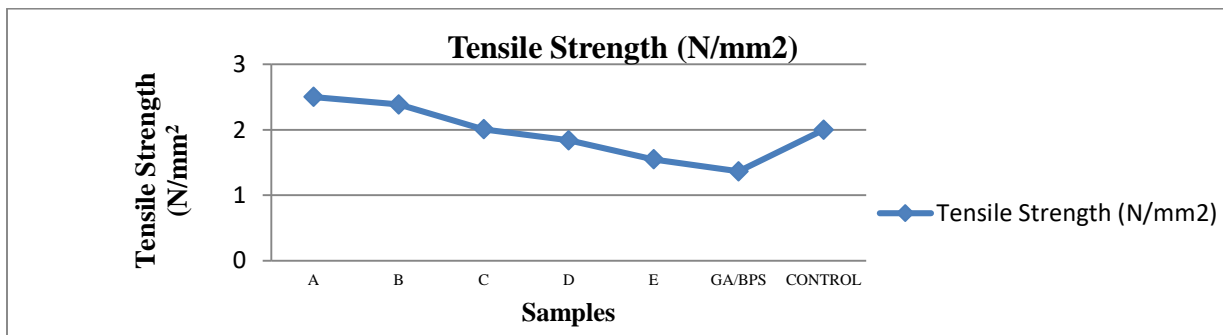


**Figure: 1: Graph of Tensile Strength of Test Samples**

The tensile test results of the gum Arabic/banana sap matrix reinforced with banana fibre and rice husk ash composite reveal a material with moderate strength, low stiffness, and significant flexibility. These properties make it suitable for applications where high strength is not critical, but flexibility and biodegradability are

### 3.3.2 Flexural test

The results of flexural strength of the samples are presented in Figure 2.

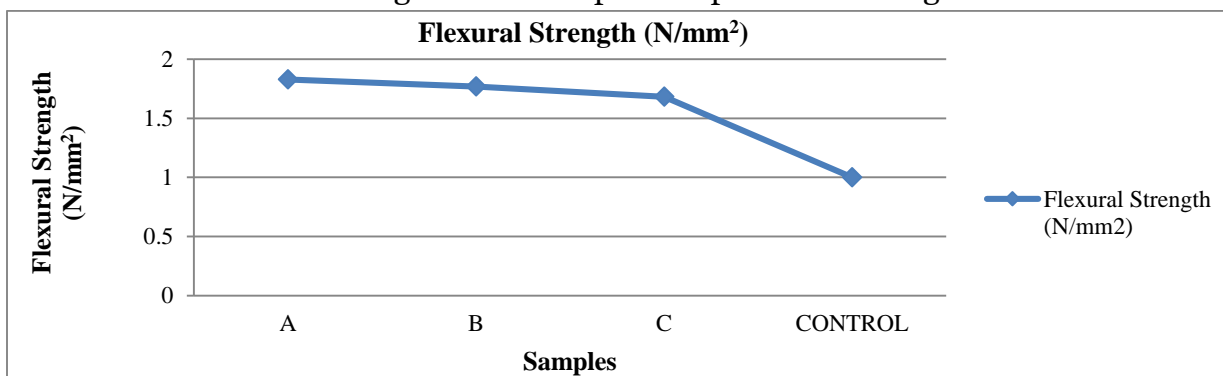


**Figure 2: Graph of Flexural Strength (N/mm²) of Flexural Test Samples**

The flexural test results show that the composite is best suited for applications requiring moderate stiffness, strength, and flexibility. The material's

important. The use of a Testometric machine ensures accurate and reliable measurement of these properties, highlighting its importance in material testing and characterization. Furthermore, the composite's composition was optimised using computer software to enhance its mechanical properties for use in an automobile headliner.

stiffness and moderate strength make it suitable for use in lightweight automobile body panels or biodegradable structural elements like headliners and other automobile interior applications.

**Danladi K. Garba, Emmanuel O. Aweda, Nuhu A. Ademoh, Fredrick Ngolemasango, Pascal A. Ubi, Akor Terngu, Lawal Kabir and Shuaibu O. Yakubu**



### 3.3.3 Hardness Test

Results of Brinell hardness (HB) test carried out on the samples are shown in Figure 3. The hardness values are in Newtons.

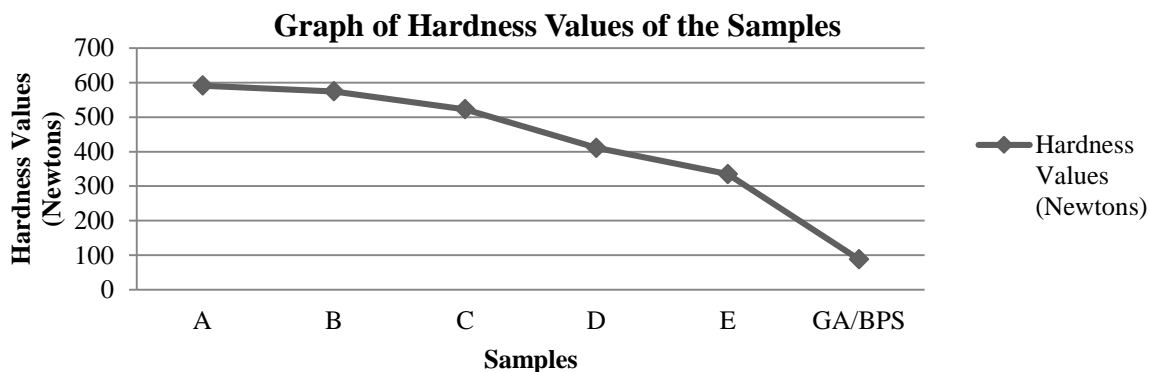


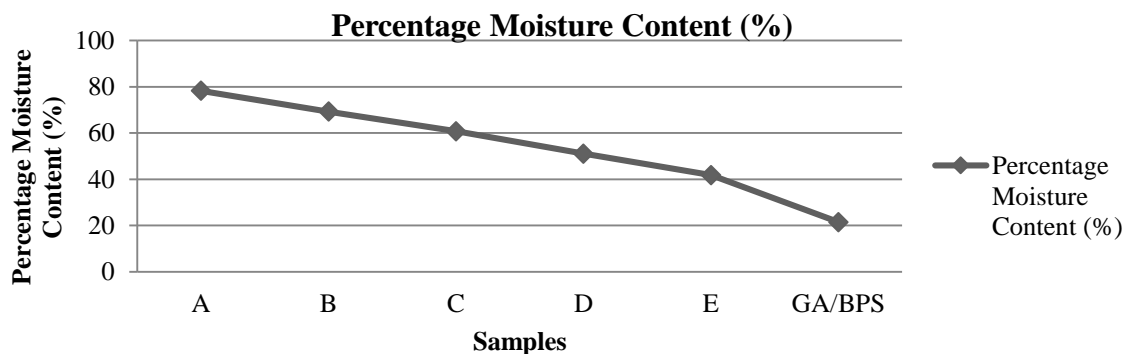
Figure 3: Hardness Test Graph of the Samples

The hardness values of the composite samples (Figure 3) displayed a clear trend that correlates with the fibre content in each sample. Sample A, which has the highest fibre content, had the highest hardness value of 591N/mm<sup>2</sup>. Conversely, sample E, with the lowest fibre content, shows the lowest hardness value of 335 N/mm<sup>2</sup>. This trend suggests that the fibre content plays a significant role in determining

the mechanical properties, particularly hardness, of the composite material.

The high hardness value of Sample A can be attributed to the increased fibre content, which likely improves the structural integrity and load-bearing capacity of the composite. The fibres act as reinforcing agents, distributing stress more effectively and resisting deformation under applied force.

### 3.4 PERCENTAGE WATER ABSORPTION (PERCENTAGE MOISTURE CONTENT)



**Danladi K. Garba, Emmanuel O. Aweda, Nuhu A. Ademoh, Fredrick Ngolemasango, Pascal A. Ubi, Akor Terngu, Lawal Kabir and Shuaibu O. Yakubu**





**Figure 4: Percentage Water Absorption (PWA)**

The water absorption results of the composite samples showed a clear trend, which is that water absorption decreases as the fiber content in the composite decreases (Figure 4). Sample A, with the highest fiber content, had the highest water absorption (78.2722%), while Sample E, with the

lowest fiber content, showed the lowest water absorption (41.8462%). This trend can be attributed to the hydrophilic nature of natural fibers, such as banana pseudostem fibers, which tend to absorb more water when present in higher quantities within the composite matrix.

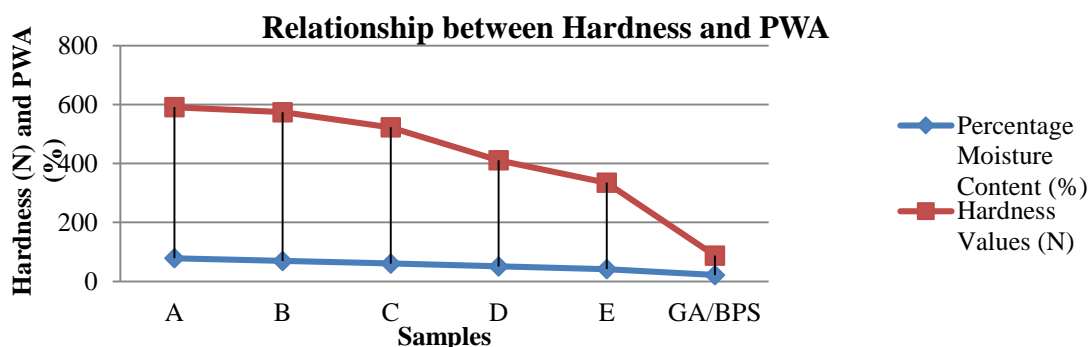


**Figure 5: Relationship between Hardness Values and PWA**

Both hardness and percentage water absorption (PWA) followed the same trend- their values increased as fiber content was increased (Figure 5). Though the trend was proportional, values of hardness were far above those of PWA. This means that the samples were harder than the rate at which they absorbed water. Control sample had the lowest hardness and PWA values.

#### 4.0 CONCLUSIONS

The experimental results conclusively show that the synergistic combination of these components yielded a material with significantly enhanced mechanical, thermographic and physical properties. The developed composite demonstrated a tensile strength of 2.5 N/mm<sup>2</sup> (compared to a control of 2.0 N/mm<sup>2</sup>), a flexural

strength of 1.9 N/mm<sup>2</sup> (control: 1.0 N/mm<sup>2</sup>), and a hardness value of 591 N/mm<sup>2</sup>. These values are superior to those of the control samples and, critically, meet or exceed the standard performance thresholds required for non-structural automotive components, particularly headliners and interior trim parts. This enhancement is attributed to the high aspect ratio and excellent mechanical properties of the BPF nanoparticles, which provide primary reinforcement; coupled with the role of RHA nanoparticles in improving matrix-filler interfacial adhesion, load distribution, and thermal stability. The gum Arabic/banana sap matrix proved to be an effective and sustainable binder, facilitating a strong interface with the natural fillers. In addition to mechanical performance, this composite system offers

**Danladi K. Garba, Emmanuel O. Aweda, Nuhu A. Ademoh, Fredrick Ngolemasango, Pascal A. Ubi, Akor Terngu, Lawal Kabir and Shuaibu O. Yakubu**



profound environmental and economic advantages. It valorizes waste products—banana pseudostem and rice husk—into high-value engineering materials, contributing to a circular economy and reducing the automotive industry's reliance on petroleum-based composites.

In conclusion, this research validates the potential of a novel, triple-hybrid bio-composite as a viable, sustainable, and high-performance alternative to conventional materials in automotive body parts. It provides a compelling blueprint for turning agricultural waste into valuable resources, paving the way for greener manufacturing practices in the automotive industry and beyond.

### **5.0 ACKNOWLEDGEMENTS**

The researchers acknowledge the financial support provided by the National Research Fund (NRF) of the Tertiary Education Trust Fund (TetFund) for this research.

### **REFERENCES**

Das, S. (2017). Life Cycle Assessment of Carbon Fiber-Reinforced Polymer Composites. *The International Journal of Life Cycle Assessment*, 22(1), 79-92.

Faruk, O., Bledzki, A. K., Fink, H. P., & Sain, M. (2012). Biocomposites Reinforced with Natural Fibers: 2000–2010. *Progress in Polymer Science*, 37(11), 1552–1596.

Pickering, K. L., Efendy, M. G. A., & Le, T. M. (2016). A Review of Recent Developments in Natural Fibre

We sincerely appreciate the access granted to required equipment and resources by:

1. The Department of Mechanical Engineering, Nigerian Defence Academy, Kaduna.
2. Spectral Laboratories Services, Kurmin Mashi, Kaduna.
3. The Federal University of Technology, Minna.
4. The Department of Chemical Engineering, Kaduna Polytechnic, Kaduna.

We also extend our profound appreciation to the technical staff of the Mechanical Engineering Workshop and the laboratories of the Department of Mechanical Engineering, Nigerian Defence Academy and Kaduna for their valuable contributions.

Composites and Their Mechanical Performance. *Composites Part A: Applied Science and Manufacturing*, 83, 98–112.

Khalil, H. P. S. A., Bhat, A. H., & Yusra, A. F. I. (2012). Green Composites from Sustainable Cellulose Nanofibrils: A Review. *Carbohydrate Polymers*, 87(2), 963–979.

Ali, B. H., Ziada, A., & Blunden, G. (2009). Biological Effects of Gum Arabic: A

**Danladi K. Garba, Emmanuel O. Aweda, Nuhu A. Ademoh, Fredrick Ngolemasango, Pascal A. Ubi, Akor Terngu, Lawal Kabir and Shuaibu O. Yakubu**



Review of Some Recent Research. Food and Chemical Toxicology, 47(1), 1-8.

Venkateshwaran, N., & ElayaPerumal, A. (2012). Banana Fiber Reinforced Polymer Composites - A Review. Journal of Reinforced Plastics and Composites, 31(7), 455-469.

Pode, R. (2016). Potential Applications of Rice Husk Ash Waste from Rice Husk Biomass Power Plant. Renewable and Sustainable Energy Reviews, 53, 1468-1485.

Composite Materials (Department of Defense) Handbook (2002), Volume 1. Polymer Matrix Composites Guidelines for Characterization of Structural Materials, Army Research Laboratory, Weapons and Materials Research Directorate, MIL-HDBK-17-1F.

Manohar DM (2017). Testing of Composites – II, Module 5 and PEB3213 - *Polymer Composites Engineering*.